CHAPTER 3

RESULTS AND DISCUSSION

3.1) Identification of transfected CHO cell [125-127]

The cultured CHO cells were subjected to transfection with the ET_A-expression plasmid DNA using a lipofectin reagent. The efficacy of ET_A expression was shown by the competitive binding assay with a synthetic sample of ET-1 and the radiolabeled [^{125}I]-ET-1 (Fig. 3.1). The binding affinity of the transfected cell line by the agonist ET-1 was established to have a dissociation constant of K_d = 1.52 nM. The receptor density (B_{max}) of 6.3×10^5 sites/cell was estimated from a Scatchard plot [128,129]. This result indicated that ET_A receptors were successfully over-expressed in the CHO cells. The CHO cells harbouring ET_A were fixed by treatment with formaldehyde. A fused-silica capillary column (200 μm inner diameter) was prior charged with poly-L-lysine, and then purged with the cross-linked CHO cells. After capping the exposed portion of poly-L-lysine with fetal bovine serum, the cell-immobilized capillary column was furnished and ready for the ACE study. It was estimated that about 1-3 cells were attached to the capillary cross-section.

Among several possible candidates of base material, poly-L-lysine turned out to exhibit a superb adhesive property for the immobilization of cells on the capillary column. The whole-cell immobilized capillary column was easily prepared, and no obvious decomposition was found on storage with PBS buffer at room temperature for seven days.

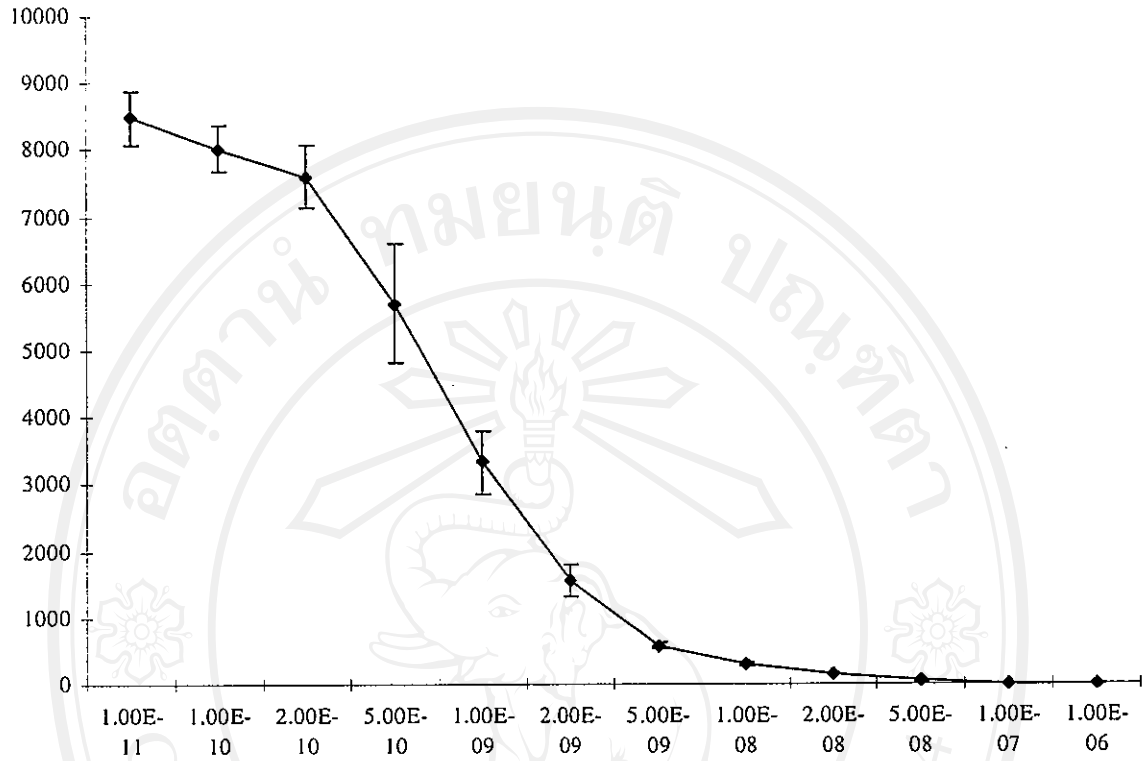

Figure 3.1 I^{125} endothelin 1 binding assay was performed with a synthetic endothelin 1 (ET-1). The binding affinity of transfected CHO cell-line was established with Kd = 1.516 nM, and the Bmax was estimated at 6.29 x 105 sites/cell.

3.2) Validation of peptide ligands

In order to validate our ACE method, we first analyzed three known peptide ligands of ET_A receptor: an ET-1 *C*-terminal fragment ET-1(16-21) that contains six amino acid residues[130,131] and two cyclic pentapeptides BQ123 [132] and JKC302[133,134]. The behavior of these ligands on three different capillary columns was examined, *i.e.* an uncoated column, a column coated with poly-L-lysine, and a column coated with fixed ET_A-overexpressing CHO cells. The first set of electrophorograms indicated that these three compounds were poorly resolved on an uncoated column, as one would

expect. The eluting order of three peptides on the poly-L-lysine-coated column differs from that on the cell-coated column, presumably due to the random electrostatic interactions exerted by poly-L-lysine on the peptide analytes. Complete separation of the mixture of ET-1(16-21), BQ123 and JKC302 was achieved on a capillary column with the stationary phase of immobilized ET_A-overexpressing CHO cells (Fig. 3.2). The cyclopeptide JKC302 with the longest retention time on the cell-coated column should exhibit the highest affinity toward ET_A, whereas the hexapeptide ET-1(16-21) with the shortest retention time should have the least affinity.

The speculation of relative affinity JKC302 > BQ123 > ET-1(16-21) as deduced from the ACE experiment was further supported by the functional assay of their antagonistic potency against ET-1. It is well known that the binding of ET-1 with ET_A will trigger an increase of intracellular calcium concentration. A control experiment (Fig. 3.3a) was performed by treatment of ET-1 in 10^{-7} M to the ET_A over-expressing CHO cells, which were prior incubated with a calcium chelating agent fura-2 applied as its penta(acetoxymethyl) ester [135]. The $[Ca^{2+}]_i$ change was monitored by a ratiometric method using dual excitations at 340 and 380 nm wavelengths, and the fluorescence emission at 505 nm was measured. As shown in Fig. 3.3a, the treatment with ET-1 induced a great degree of $[Ca^{2+}]_i$. When a mixture of JKC302 (10^{-6} M) and ET-1 (10^{-7} M) was used in such functional assay, the ET-1 induced $[Ca^{2+}]_i$ change was entirely suppressed (Fig. 3.3b). The degree of inhibition against the ET-1 induced $[Ca^{2+}]_i$ can serve as a measure of the potency of an antagonist. By comparison of the transient $[Ca^{2+}]_i$ assays (Fig. 3.3b-d), the relative potency JKC302 > BQ123 > ET-1(16-21) in ET_A antagonism is in good agreement with that derived by the eluting order on the capillary column coated with whole cells.

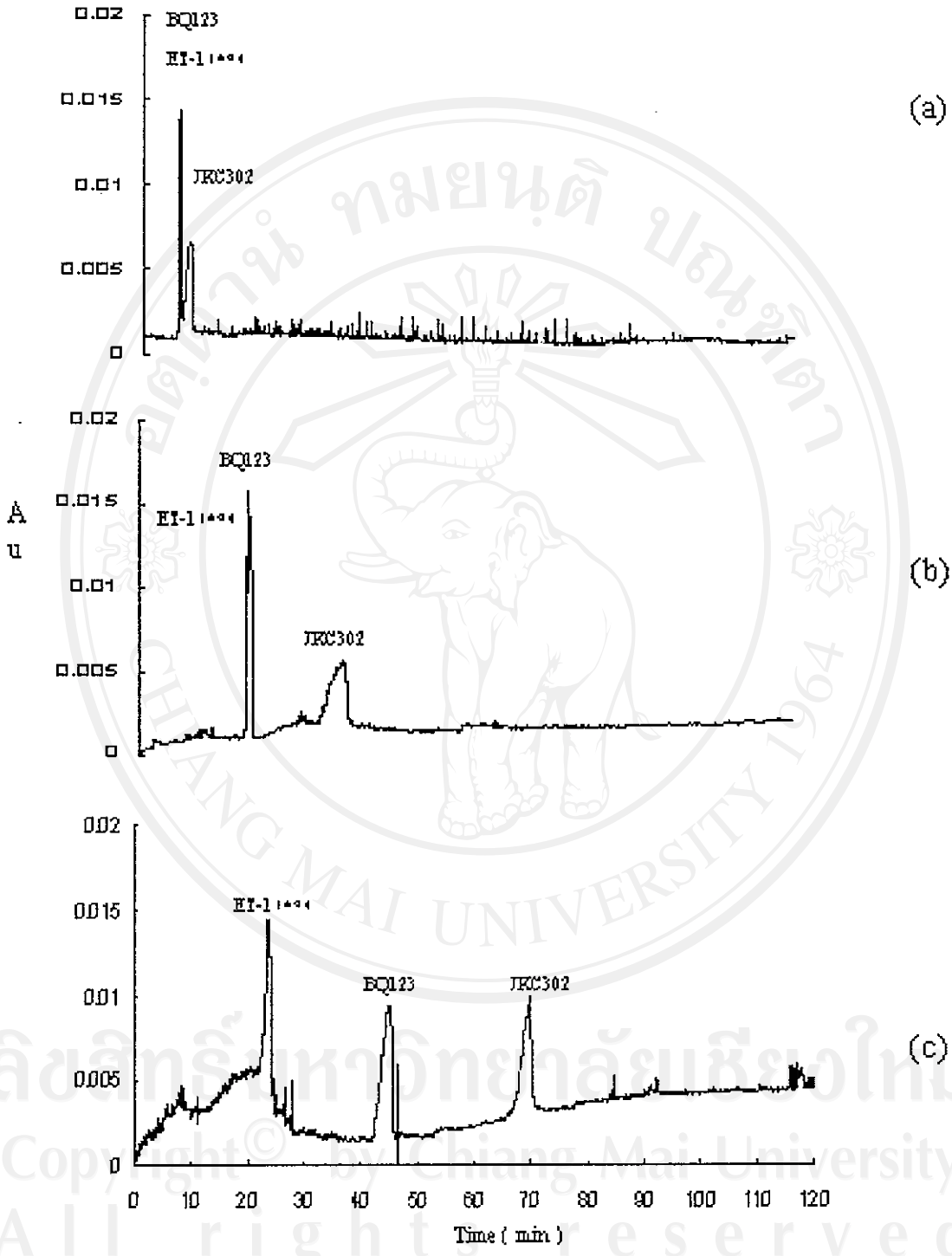

Figure 3.2 Affinity capillary electrophoresis of peptides JKC 302, BQ123, and ET-1(16-21) on a column: (a) uncoated column; (b) coated poly-L-Lysine; (c) coated with fixed ET_A-overexpressing CHO cells. The background electrolyte is 1 mM PBS and the absorbance detector is held at 214 nm. Au, arbitrary unit.

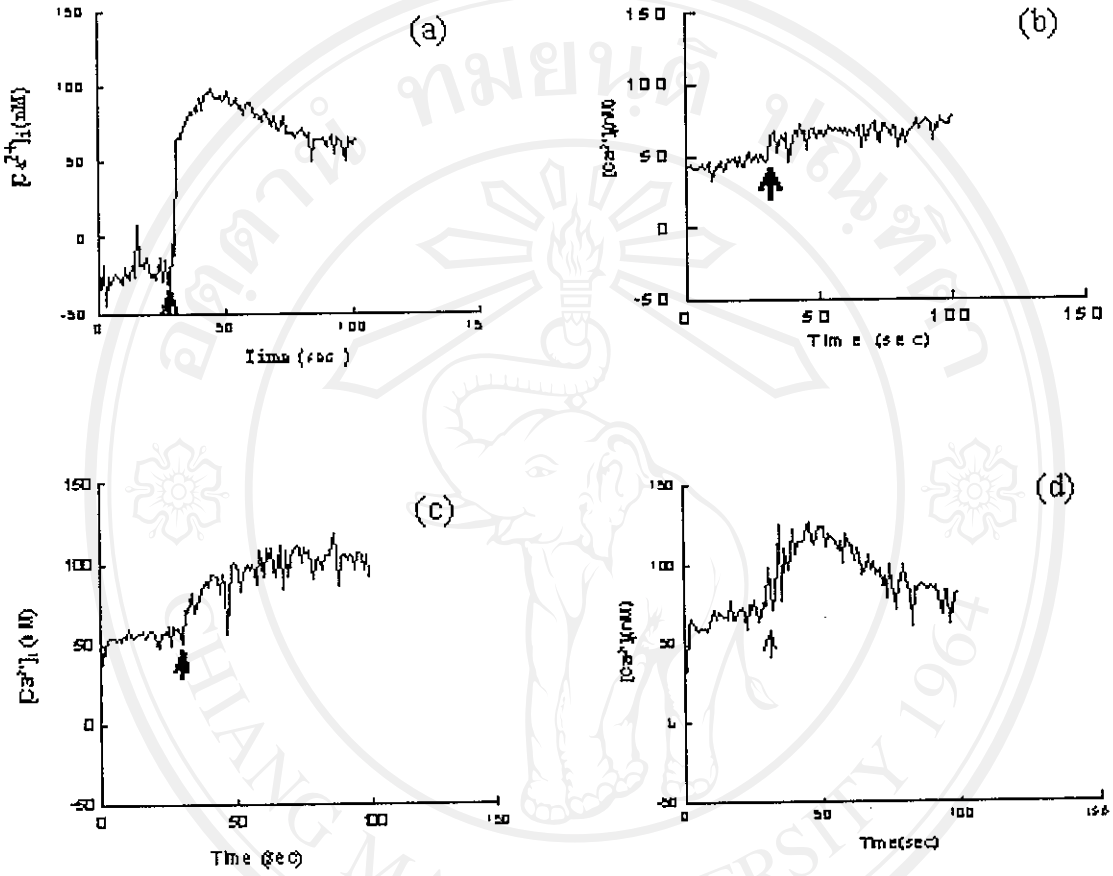

Figure 3.3 Fluorescence measurements of intracellular calcium concentration ($[Ca^{2+}]i$) by addition of tested samples (as shown by the arrow) to the ETA-overexpressing CHO cells in the presence of fura-2. The induced $[Ca^{2+}]i$ change is taken as a measure of antagonist potency against ET-1: (a) control experiment with addition of ET-1 (10^{-7} M), (b) treatment with a mixture of JKC302 (10^{-6} M) and ET-1 (10^{-7} M), (c) treatment with a mixture of BQ123 (10^{-6} M) and ET-1 (10^{-7} M), and (d) treatment with a mixture of ET-$1^{(16-21)}$ (10^{-6} M) and ET-1 (10^{-7} M).

3.3) Validation of nonpeptide ligands

Our present whole-cell coating ACE method is not limited to peptide antagonists; it is also applicable for screening non-peptide antagonist molecules. For example, 1,3-diarylindane-2-carboxylic acid SB209670 is a very potent ET_A antagonist against ET-1 . The molecular computations together with the bioassay of a series of derivatives indicated that SB209670 bears a carboxyl group at the 2-position to mimic the carboxylic terminal of ET-1, and two aryl groups at 4- and 9-positions to mimic the aromatic residues of Tyr-13 and Phe-14. On the basis of this structural protocol, carbazolothiophene-2-carboxylic acid JMF310 was designed as a possible ET_A antagonist, and indenecarboxylate ester YHK891 was also examined for comparison. Indeed, SB209670 that strongly inhibited the ET-1 induced $[Ca^{2+}]_i$ increase (Fig. 3.5b) also showed a very long retention time on the whole-cell immobilized capillary column (Fig. 3.4), as a consequence of its high affinity toward the surface endothelin receptors of the transfected CHO cells. The modest antagonist potency of JMF310 (Fig. 3.5c) was also reflected in the ACE elution profile. On contrary, the YHK891 sample having only a marginal inhibitory effect against ET-1 (Fig. 3.5d) was rapidly eluted out from the whole-cell coating column.

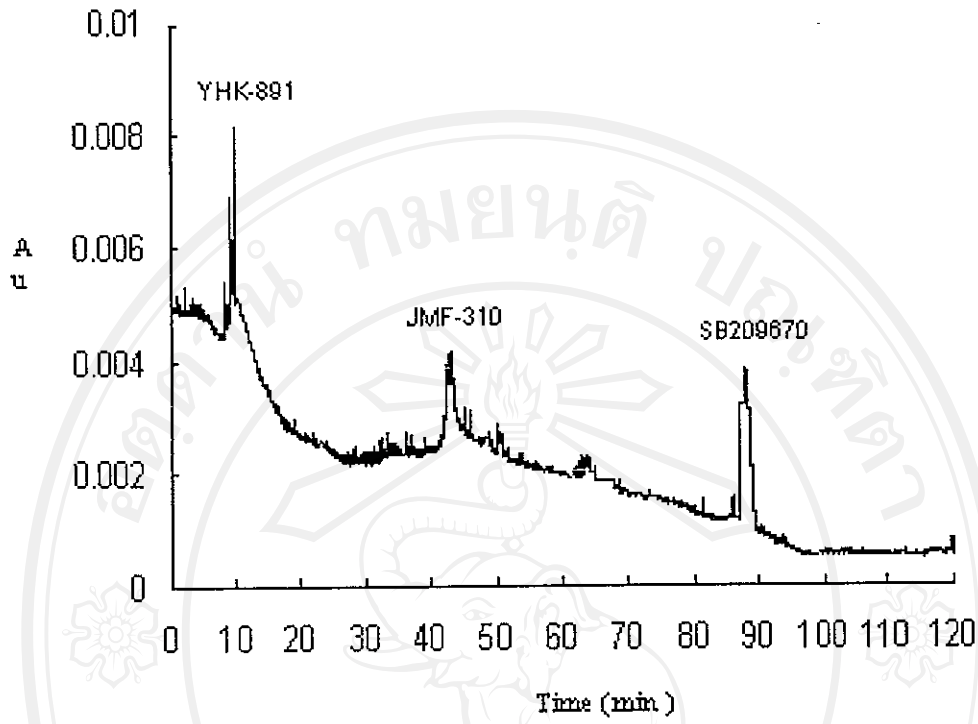

Figure 3.4 Affinity capillary electrophoresis of a mixture of SB209670, JMF310 and YHK891 on a capillary column coated with fixed ET_A-overexpressing CHO cells. The background electrolyte is 1 mM PBS and the absorbance detector is held at 214 nm. Au, arbitrary unit.

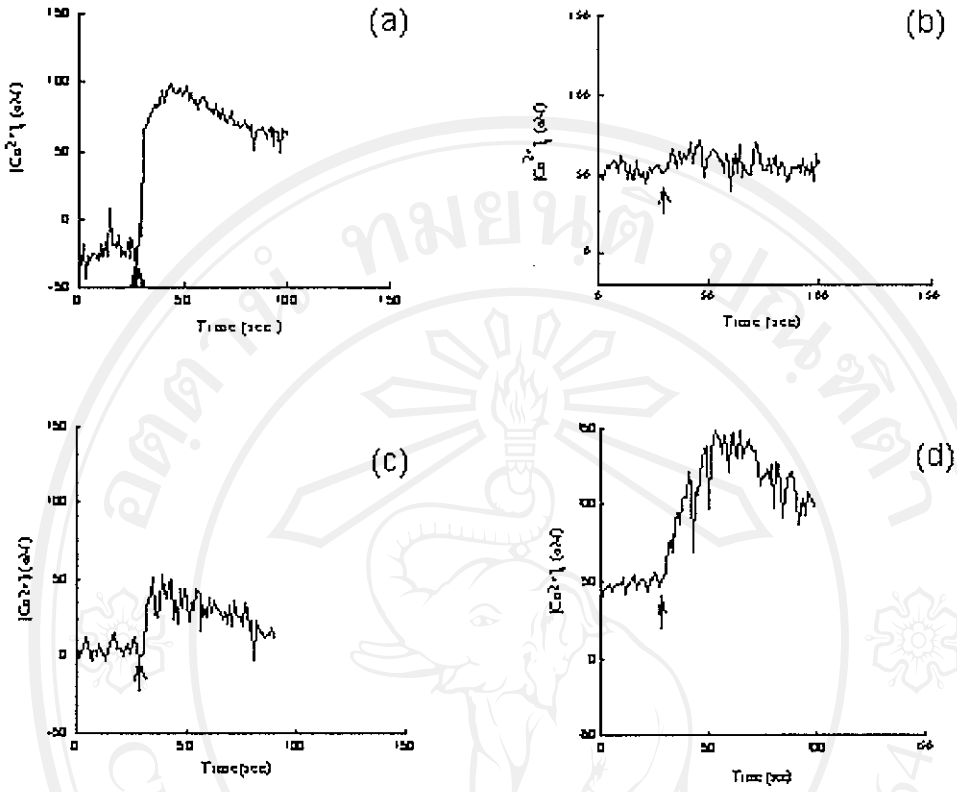

Figure 3.5 Fluorescence measurements of intracellular calcium concentration ($[Ca^{2+}]i$) by addition of tested samples (as shown by the arrow) to the ETA-overexpressing CHO cells in the presence of fura-2. The induced $[Ca^{2+}]i$ change is taken as a measure of antagonist potency against ET-1: (a) control experiment with addition of ET-1 (10^{-7} M), (b) treatment with a mixture of SB209670 (10^{-6} M) and ET-1 (10^{-7} M), (c) treatment with a mixture of JMF310 (10^{-6} M) and ET-1 (10^{-7} M), and (d) treatment with a mixture of YHK891 (10^{-6} M) and ET-1 (10^{-7} M).

3.4) Validation of active herbal components

In addition to the rationally designed molecules, the random screening of active components can also be achieved by the whole-cell ACE method. Along this line, we have selected several active herbal components that are known to possess bioactivities related to vascular dilation or signal transduction. From the ACE study, we

found that an anti-platelet agent, Magnolol [136,137], might function as a new lead compound against ET-1 in ET_A receptor binding. Magnolol is the 2,2′-dimer of 4-allylphenol. As shown in the profiles of ACE analysis (Fig. 3.6) and $[Ca^{2+}]_i$ assay (Fig. 3.7), Magnolol is a stronger ET_A antagonist than its structural isomer, Honokiol [138]. Geniposide [139], an iridoid glucoside that exhibits neuritogenic effect on PC12h cells and enhanced responses of cells to carbachol in terms of cytoplasmic free-calcium concentration, turned out to have a temperate binding affinity and modest antagonistic activity against ET-1.

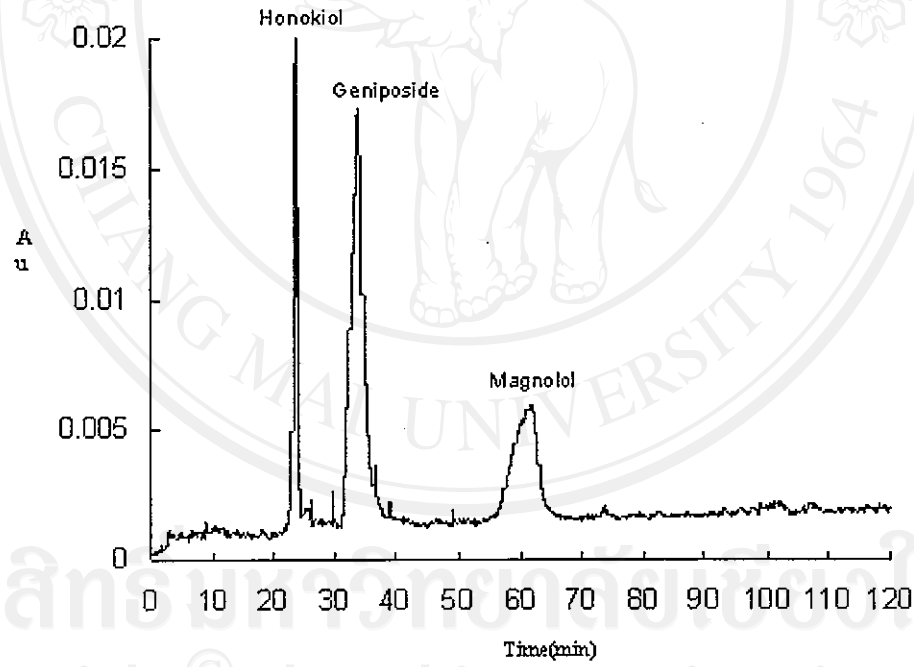

Figure 3.6 Screening of Chinese herbal active components Magnolol, Honokiol and Geniposide by affinity capillary electrophoresis on a capillary column coated with fixed ETA-overexpressing CHO cells. The background electrolyte is 1 mM PBS and the absorbance detector is held at 214 nm. Au, arbitrary unit.

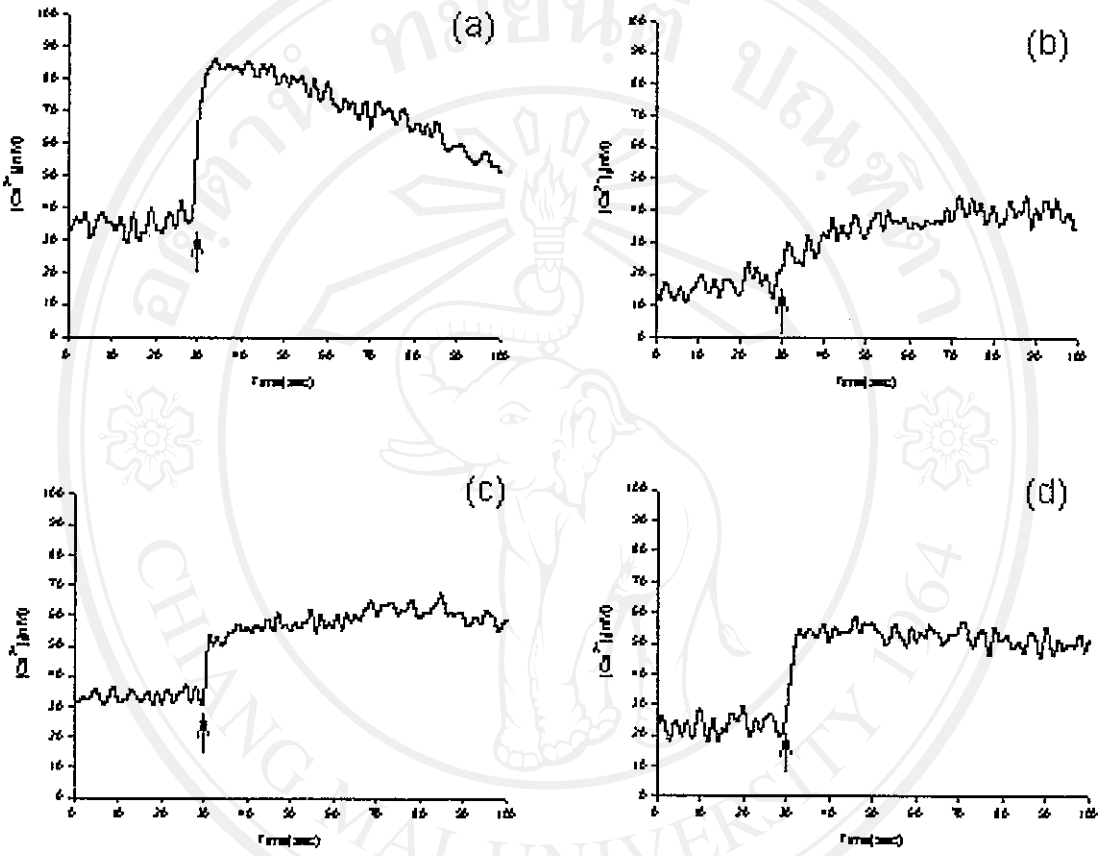

Figure 3.7 Fluorescence measurements of intracellular calcium concentration ([Ca2+]i) by addition of tested samples (as shown by the arrow) to the ETA-overexpressing CHO cells in the presence of fura-2. The induced [Ca2+]i change is taken as a measure of antagonist potency against ET-1: (a) control experiment with addition of ET-1 (10-7 M), (b) treatment with a mixture of Magnolol (10-6 M) and ET-1 (10-7 M), (c) treatment with a mixture of Geniposide (10-6 M) and ET-1 (10-7 M), and (d) treatment with a mixture of Honokiol (10-6 M) and ET-1 (10-7 M).

3.5) ET_A antagonists nonpeptides(I):Carbazolothiophene-2-carboxylic acid derivatives

The interaction of ET-1 with endothelin receptor is known to trigger an increase of intracellular Ca^{2+} concentration ($[Ca^{2+}]_i$) as the consequence of multistep biological events initiated by G-protein. To evaluate the potency of an endothelin receptor antagonist, one can measure its inhibitory ability against the ET-1 induced $[Ca^{2+}]_i$ change. According to the reported experimental protocol, Chinese hamster ovary (CHO-K1) cells were transfected with the rat ET_A-expression plasmid DNA using lipofectin reagent. The ET_A overexpression CHO-K1 cells were prior incubated with calcium chelating agent fura-2 applied as its penta(acetoxymethyl) ester, and then treated with ET-1 in 10^{-7} M. The $[Ca^{2+}]_i$ increase was monitored at 510-nm fluorescence emission by a ratiometric method using dual excitations at 340 and 380 nm wavelengths. This increment of functional assay was taken as the standard value (100%) to assess the inhibitory potency of compounds 7-22 against the ET-1 binding with receptor. By addition of the test sample 7 (10^{-6} M) along with ET-1 (10^{-7} M), only 30 ± 5% increment of $[Ca^{2+}]_i$ was observed (a mean value of three measurements), equivalent to ~ 70% inhibition. By comparisons with the known ET_A antagonists, 10^{-6} M of SB209670 completely inhibited the ET-1 induced $[Ca^{2+}]_i$, whereas BQ123 showed ~ 60% inhibition under our assay conditions. Accordingly, compounds 9, 10, 12, 13 and 18 showed high inhibition (> 75%) at 10^{-6} M. Compounds 7, 11, 15 and 19 showed medium inhibition (50-70%), whereas compounds 14, 16, 17 and 20-22 showed low inhibition. Among our examined samples, compound 18 appeared to be the best ET-1 antagonist with IC_{50} ~ 10 nM. In comparison, SB209670 is an even more potent antagonist showing ~ 85% inhibition at 10 nM.

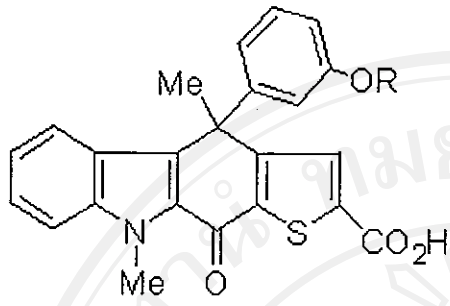

11 R = Me
12 R = CH_2CO_2H
13 R = $(CH_2)_3CO_2H$

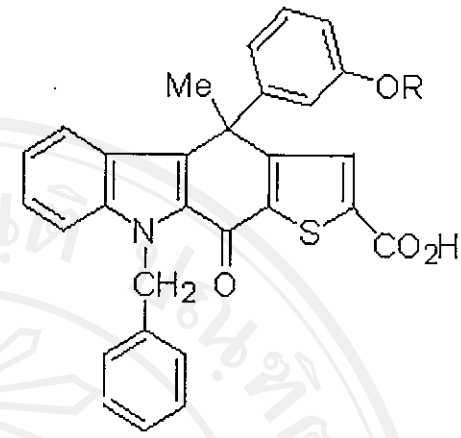

14 R = Me
15 R = H
16 R = CH_2CO_2H

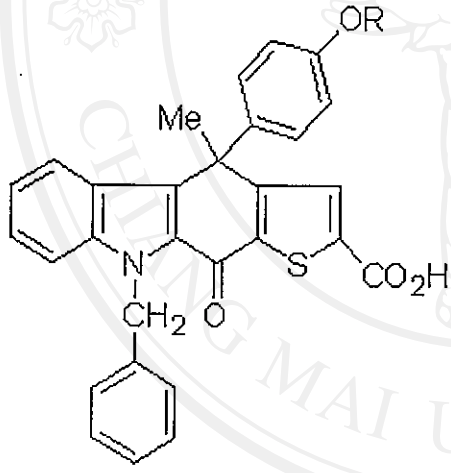

17 R = Me
18 R = H
19 R = CH_2CO_2H

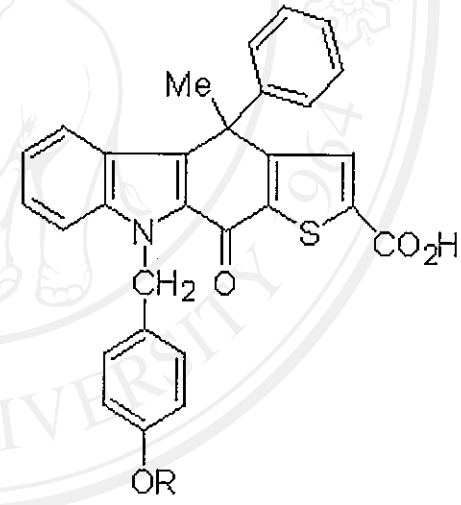

20 R = Me
21 R = H
22 R = CH_2CO_2H

Figure 3.8 A series of carbazolothiophenes 11-12 were similarly prepared, initially by the SmI_2-promoted three-component coupling reactions with appropriate partner substrates. 11-13 bearing MeO, CH_2CO_2H or $(CH_2)_3CO_2H$, 14-19 with the (substituted) benzyl groups on the nitrogen atoms were prepared, 20-22 are analogues of 17-19 having the substituents switched over.

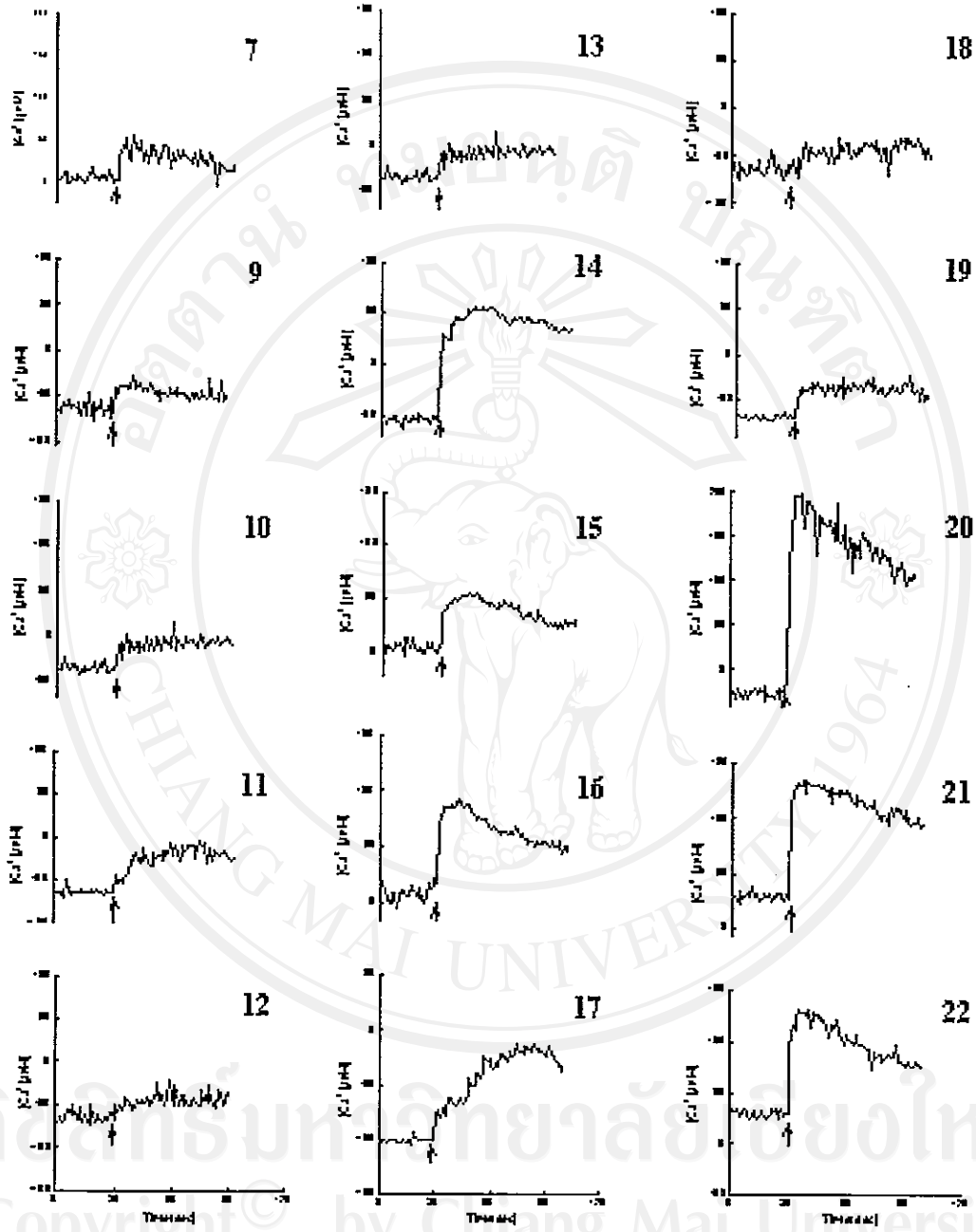

Figure 3.9 Fluorescence measurements of intracellular calcium concentration ($[Ca^{2+}]_i$) by addition of tested samples to the ET_A-overexpressing CHO cells in the presence of fura-2. The induced $[Ca^{2+}]_i$ change is taken as a measure of antagonist potency against ET-1: treatment with a mixture of antagonists (7-22 of Carbazolothiophene-2-carboxylic acid derivatives, 10^{-6} M) and ET-1 (10^{-7} M).

3.6) ET_A antagonists nonpeptides(II): 1,4-benzodiazepine-2,5-diones derivatives

3.6.1) Liquid-phase synthesis

This new series of 1,4-Benzodiazepine-2,5-diones had also been evaluated, and the other conclusion derived from the above result of inhibition was mentioned as comparing the series of N-4 side-chained benzylated compounds with the series of N-1 side-chained benzylated compounds: 24 to 25, 26 to 27, 28 to 29, 30 to 31, 32 to 33, the former ones exhibited the better inhibition.(Fig. 3.10) The possible reason might be explained as the optimised distance between the C-3 side-chain and the aromatic ones.

The 1,4-benzodiazepine-2,5-diones with the anisole or phenol moiety, 26, show the significant inhibition due to the oxygen atom of the anisole or phenol moiety, and the ester may chelate zinc ion in physiological conditions, even in the absence of carboxylate. The target dicarboxylate, 32 and 33, did not exhibit the anticipated inhibition which might be caused by the unavailable length of the aromatic side chain.

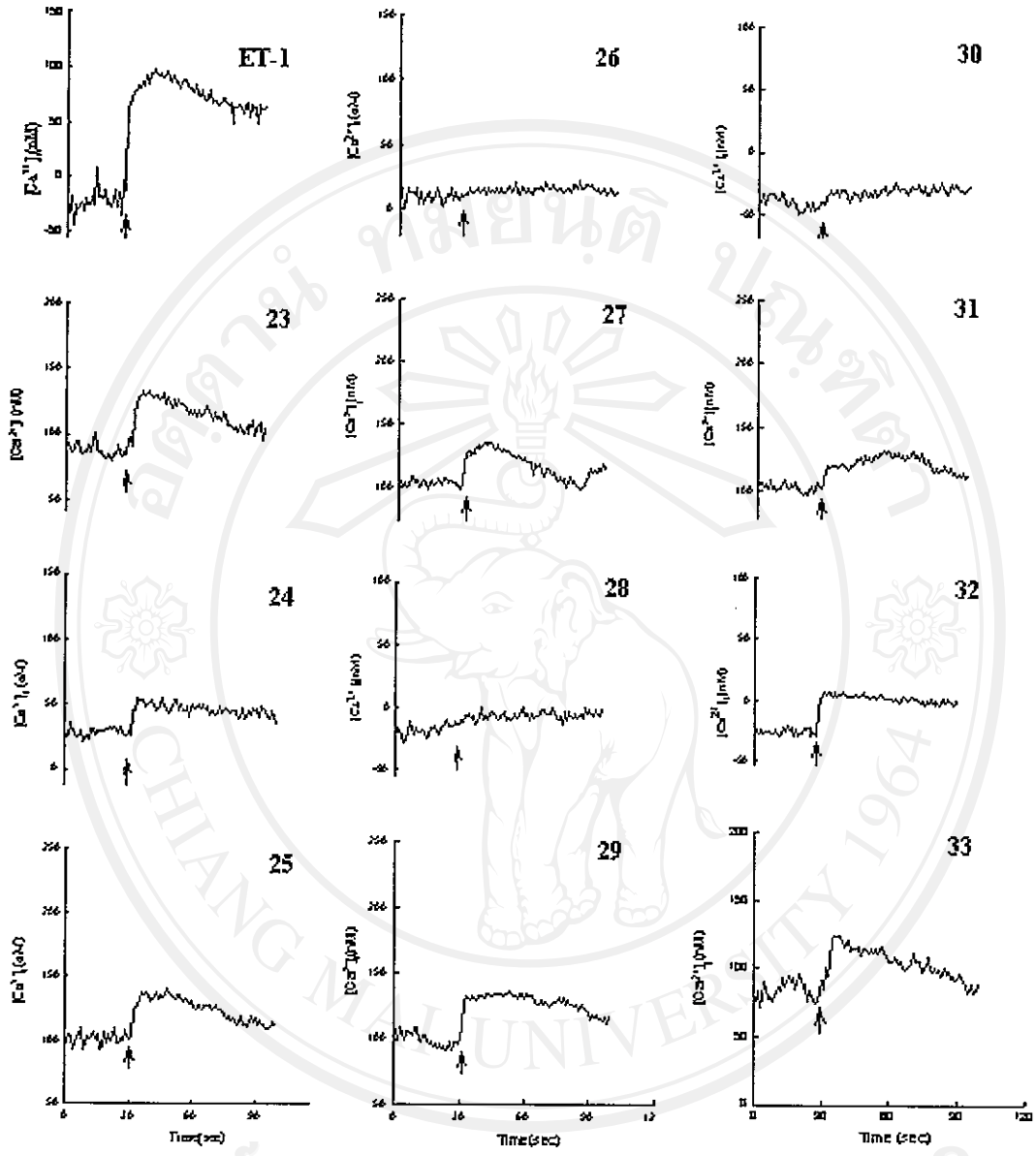

Figure 3.10 Fluorescence measurements of intracellular calcium concentration ($[Ca^{2+}]_i$) by addition of tested samples to the ET_A-overexpressing CHO cells in the presence of fura-2. The induced $[Ca^{2+}]_i$ change is taken as a measure of antagonist potency against ET-1: treatment with a mixture of antagonists (23-33 of 1,4-Benzodiazepine-2,5-diones ,10^{-6} M) and ET-1 (10^{-7} M).

3.6.2) Polyethylene resin-bound liquid-phase synthesis

This new series of 1,4-Benzodiazepine-2,5-diones had also been evaluated, and the other conclusion derived from the above result of inhibition was mentioned as the series of N-4 side-chained benzylated compounds with the series of N-1 side-chained benzylated compounds:34-61, the former ones exhibited the better inhibition. (Fig. 3.11)

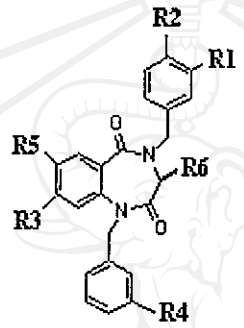

	R1	R2	R3	R4	R5	R6	Inhiby.%
34	OCH_2COOH	H	H	H	H	CH_2COOH	27
35	OCH_2COOCH_3	H	H	H	H	CH_2COOH	53
36	OCH_2COOCH_3	H	H	OCH	H	CH_2COOH	64
37	H	OCH_2COOCH_3	H	H	H	CH_2COOH	58
38	H	OCH_2COOCH_3	H	OCH	H	CH_2COOH	75
39	OCH	H	Cl	H	H	CH_2COOH	63
40	OCH	H	$NHCH_2C_6H_5$	H	H	CH_2COOH	75
41	OCH	H	NH_2	H	H	CH_2COOH	81
42	OCH	H	$NHCOCH_2Br$	H	H	CH_2COOH	76
43	OCH	H	$NHCOCF_3$	H	H	CH_2COOH	100
44	OCH	H	H	$O(CH_2)C=CH_2$	H	CH_2COOH	36
45	OCH	H	H	H	Cl	CH_2COOH	100
46	OCH	H	H	$[O(CH_2)_2]_2NCl$	Cl	CH_2COOH	43
47	OH	H	Cl	H	H	CH_2COOH	81
48	H	COOCH	H	H	H	CH_2COOH	55
49	H	COOH	H	H	H	CH_2COOH	0
50	OCH_2COOCH_3	H	H	H	H	$CH(CH_3)_2$	80
51	OCH_2COOCH_3	H	H	OCH	H	$CH(CH_3)_2$	85
52	H	OCH_2COOCH_3	H	H	H	$CH(CH_3)_2$	72
53	H	OCH_2COOCH_3	H	OCH	H	$CH(CH_3)_2$	73
54	OCH_2COOCH_3	H	OCH	H	OCH	CH_2COOH	72
55	OCH_2COOCH_3	H	OCH	OCH	OCH	CH_2COOH	58
56	H	OCH_2COOCH_3	OCH	H	OCH	CH_2COOH	75
57	OCH_2COOCH_3	H	OCH	OCH	OCH	CH_2COOH	50
58	H	OCH_2COOCH_3	OCH	OCH	OCH	CH_2COOH	60
59	OCH_2COOCH_3	H	OCH	H	OCH	$CH(CH_3)_2$	90
60	H	OCH_2COOCH_3	OCH	H	OCH	$CH(CH_3)_2$	82
61	H	OCH_2COOCH_3	OCH	OCH	OCH	$CH(CH_3)_2$	81

Figure 3.11 A series of 1,4-Benzodiazepine-2,5-diones 34-61 were similarly prepared And fluorescence measurements of intracellular calcium concentration ($[Ca^{2+}]_i$) .